

New Application of a Sona Transition Unit: Observation of Direct Transitions Between Quantum States With Energy Differences of 10 neV and Below

Chrysovalantis S. KANNIS^{1,2}, Ralf ENGELS¹, Christoph HANHART^{1,3}, Helmut SOLTNER⁴, Lukas HUXOLD⁵, Kirill GRIGORYEV¹, Andreas LEHRACH^{1,2,6}, Markus BÜSCHER^{5,7}, and Thomas SEFZICK¹

¹*Institut für Kernphysik, Forschungszentrum Jülich, Jülich, Germany*

²*III. Physikalisches Institut B, RWTH Aachen University, Aachen, Germany*

³*Institute for Advanced Simulation, Forschungszentrum Jülich, Jülich, Germany*

⁴*Zentralinstitut für Engineering, Elektronik und Analytik, Forschungszentrum Jülich, Jülich, Germany*

⁵*Institut für Laser- und Plasmaphysik, Heinrich-Heine-Universität Düsseldorf, Düsseldorf, Germany*

⁶*JARA-Fame, Forschungszentrum Jülich and RWTH Aachen University, Aachen, Germany*

⁷*Peter-Grünberg Institut, Forschungszentrum Jülich, Jülich, Germany*

E-mail: c.kannis@fz-juelich.de

(Received February 14, 2022)

For more than 50 years Sona transition units have been used at polarized sources to exchange the occupation numbers between “pure” hyperfine substates. For instance, hydrogen atoms in the hyperfine substate $|F = 1, m_F = +1\rangle$ are transferred into $|F = 1, m_F = -1\rangle$ when these atoms are passing a static magnetic field gradient between two opposing solenoidal magnetic fields. Thus, the magnetic field direction, i.e. the quantization axis, is rotated faster than the spin orientation can follow due to the Larmor precession.

In parallel, the atoms traveling through the zero crossing of the static magnetic field experience in their rest frame an oscillating magnetic field. This oscillation is equivalent to an external radio frequency field of frequency $f = v_{atom}/\lambda$ that can induce transitions between hyperfine substates with the energy difference $\Delta E = n \cdot h \cdot f$, where n is an integer. Here, the distance between the opposite coils determines the wavelength λ , thus the beam velocity v_{atom} can be used to manipulate the frequency f to induce transitions between quantum states with energy differences of 10 neV and below. These tiny energy differences can be found between hyperfine substates of hydrogen atoms at low magnetic fields in the Breit-Rabi diagram. Here first measurements, their interpretation and possible applications are presented.

KEYWORDS: Sona transition, hyperfine structure, static magnetic field, spectroscopy

1. Introduction

In 1967 P. G. Sona proposed a method to increase the polarization in polarized metastable hydrogen and deuterium ion sources. He designed a device nowadays called Sona Transition unit [1] that provides a static magnetic field with field direction reversal along the polarization axis. The steps of the polarization procedure are:

- (1) Consider a hydrogen/deuterium atomic beam in the $2S_{1/2}$ state moving with a velocity v of the order of $\sim 10^5$ m/s (non-thermal beam). The beam enters a region where a magnetic field $B \sim 57.5$ mT parallel to the beam direction (z -axis) is applied. An additional small transverse

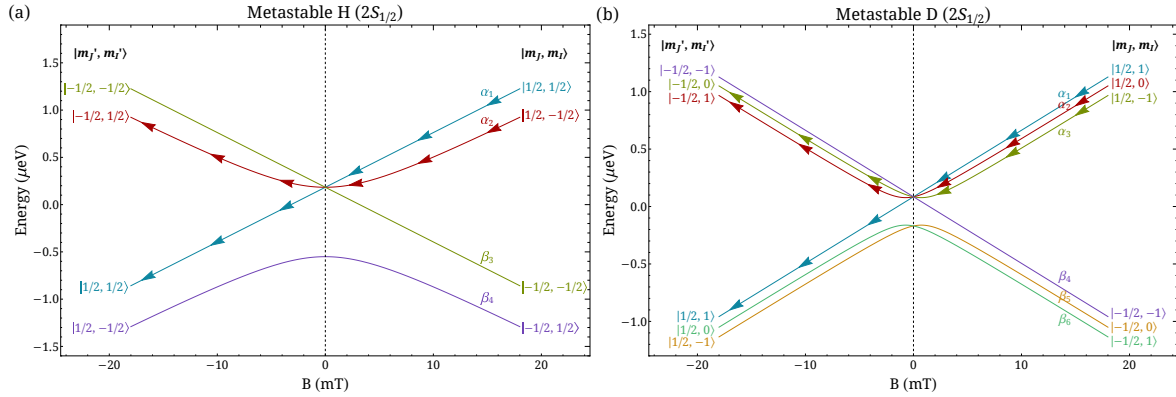


Fig. 1. Zeeman hyperfine splitting for (a) hydrogen and (b) deuterium atom in $2S_{1/2}$ state as function of external magnetic field. The arrows indicate the initial $|m_J, m_I\rangle$ and the final $|m'_J, m'_I\rangle$ substates that the eigenenergies approach for various values of magnetic field.

electric field is present. The β sublevels of the $2S_{1/2}$ state cross the sublevels of the $2P_{1/2}$ state, so that the population of the β substates is transferred to the $2P_{1/2}$ substates, which subsequently decay to the ground state. Therefore, the atoms are found only in the α sublevels with equal probability.

- (2) Next, the atomic beam enters a region with a decreasing magnetic field, but still parallel to the beam. If the decrease is slow enough (adiabatic region) each eigenstate follows the corresponding energy line (see Fig. 1). This should continue until the external field is equal to the critical field of the atom. It is $B_c = 6.34$ mT for H [2] and $B_c = 1.46$ mT for D [3]. The regions with $B \gg B_c$ are conventionally called high-field regions, and for low-field regions $B \ll B_c$ holds.
- (3) In the low-field region and particularly around the zero-crossing (see Fig. 3), we have to take into account the beam spread σ . The off-center atoms experience the radial component B_r of the magnetic field

$$B_r(z, r) = -\frac{dB_z}{dz} \cdot \frac{r}{2}, \quad (1)$$

where r is the distance from center. A particle off-axis never sees the external field going to zero, but changing direction by 180° instead. This will induce an undesirable Larmor precession around the magnetic field axis and subsequent polarization losses. To avoid this effect we apply a “sudden” (non-adiabatic) zero-crossing, so that the angular velocity of the rotation of \mathbf{B} direction is faster than the angular velocity of the Larmor precession. The zero-crossing requirements are [1]

$$\frac{eB_t^2}{2m_e v} \ll \frac{dB_z}{dz} \ll \frac{8m_e v}{er^2} \quad \text{for H} \quad \text{and} \quad \frac{eB_t^2}{3m_e v} \ll \frac{dB_z}{dz} \ll \frac{12m_e v}{er^2} \quad \text{for D}, \quad (2)$$

where m_e and e are the electron mass and unit charge, respectively.

- (4) The fulfillment of the non-adiabaticity conditions ensure that the atoms continuously stick on the energy lines while the magnetic field changes value. A Sona transition unit transfers the atoms from $|m_J, m_I\rangle$ to $|m'_J, m'_I\rangle$ states shown in Fig. 1. The (vector) nuclear polarization is 100% for H atoms (Fig. 1(a)) and 2/3 for D atoms (Fig. 1(b)). The tensor polarization is 0, but an additional electrostatic field at B , here $B \sim -57.5$ mT, quenches the α_1 state, yielding 1/2 vector polarization and $-1/2$ tensor polarization.

The concept of Sona transitions is simple and straightforward to implement in a great variety of experiments. However, during studies with ground state hydrogen atoms in the RHIC OPPIS (Optically Pumped Polarized Ion Source), oscillations in polarization for certain fields were observed [4].

These were simulated by a code developed at INR, Moscow [5], but only the loss of polarization was in a good agreement with the measured signal [6]; the number and the position of the oscillations were not sufficiently described. A similar effect was also observed with metastable hydrogen atoms [7, 8] within the BoB (bound beta-decay) experiment [9, 10]. Therefore, we investigate Sona transitions in more detail. Here, we report on the implementation of Sona transitions in a metastable hydrogen beam.

2. Experimental Setup

The experimental setup consists of components of a Lamb-shift polarimeter [11]. Figure 2 shows a sketch of the experimental setup. First, H_2 molecules are ionized in an electron-impact ionizer and the resulting ions are accelerated to 1-2 keV. Next, a Wien filter acts as a velocity and mass filter, allowing only the protons with a definite velocity to pass through. These protons form metastable hydrogen atoms via charge exchange with Cs vapor. Then, the atoms in the $\alpha_{1,2}$ are transmitted by the first spinfilter and enter the Sona transition unit which provides a static magnetic field, as shown in Fig. 3. If the atoms are prepared in the α_1 state, they should be transferred to β_3 due to the inversion of the external field direction, i.e. spins antiparallel to the magnetic field of the second spinfilter.

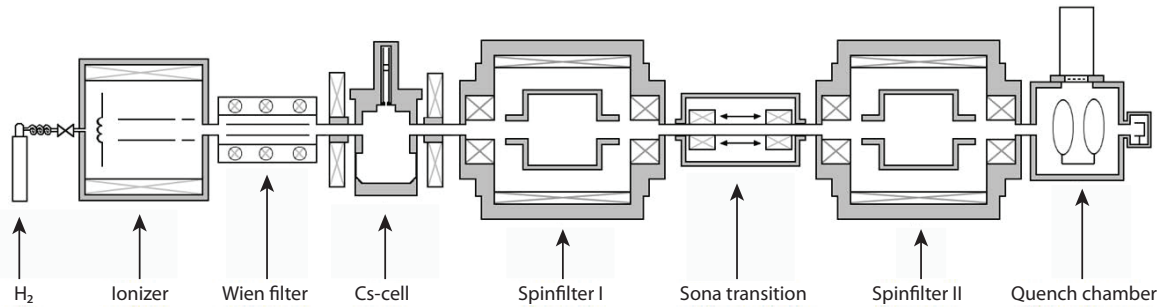


Fig. 2. Experimental setup. Figure adapted from [12].

Since a spinfilter transmits only atoms in the α states, no atoms are expected to reach the quenching chamber. However, as the recorded signals show, some atoms are found in the α states and are quenched into the ground state by the Stark effect in a strong electric field (at the quenching chamber) producing Lyman- α photons, which are registered as function of the current of the Sona coils. The occupation numbers of α_1 and α_2 states for different values of current are shown in Fig. 4.

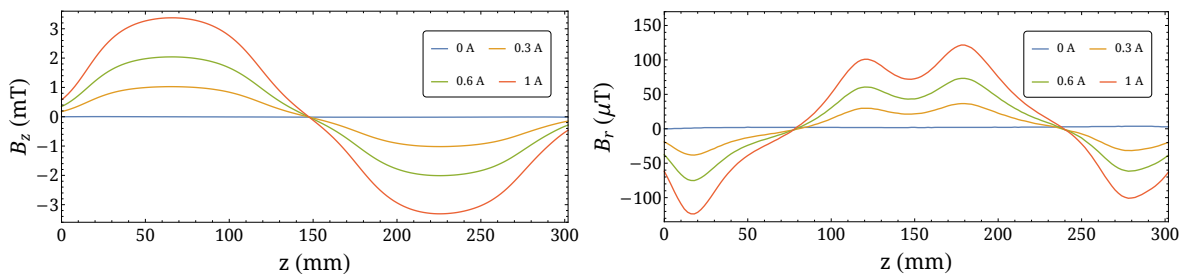


Fig. 3. Measured magnetic field components for different currents in the Sona coils. The radial component B_r is measured at a distance $r = 3$ mm from the beam axis z .

3. Theoretical Description

The hydrogen atoms are moving on a straight path with a constant velocity, so we choose to study them in their rest frame. Consequently, the spatial change of the magnetic field is experienced as a temporal one by the atoms. The effective Hamiltonian is

$$\begin{aligned} H(t) &= A\mathbf{I} \cdot \mathbf{J} - (g_J\mu_B\mathbf{J} + g_I\mu_N\mathbf{I}) \cdot \mathbf{B}(t) \\ &= H_0 + V(t), \end{aligned} \quad (3)$$

where H_0 corresponds to the unperturbed term and $V(t)$ to the external time-dependent perturbation. A is the hyperfine structure constant, g_J is the electron g -factor, g_I is the proton g -factor, and $\mu_{B,N}$ are the Bohr and nuclear magneton, respectively. Following the steps of time-dependent perturbation theory (details can be found elsewhere [12]) we obtain a system of four coupled first order differential equations

$$i\hbar \frac{\partial c_k(t)}{\partial t} = \sum_{j=1}^4 c_j(t) e^{-i(E_j - E_k)t/\hbar} \langle k|V(t)|j \rangle, \quad (4)$$

which are solved numerically. The calculated relative probabilities $|c_1(t)|^2$ and $|c_2(t)|^2$ are shown with colored curves in Fig. 4. They are evaluated for a hydrogen beam moving with a velocity $v = 4.95 \times 10^5$ m/s ($E_{beam} = 1.28$ keV) and a Gaussian profile with a spread $\sigma = 5$ mm.

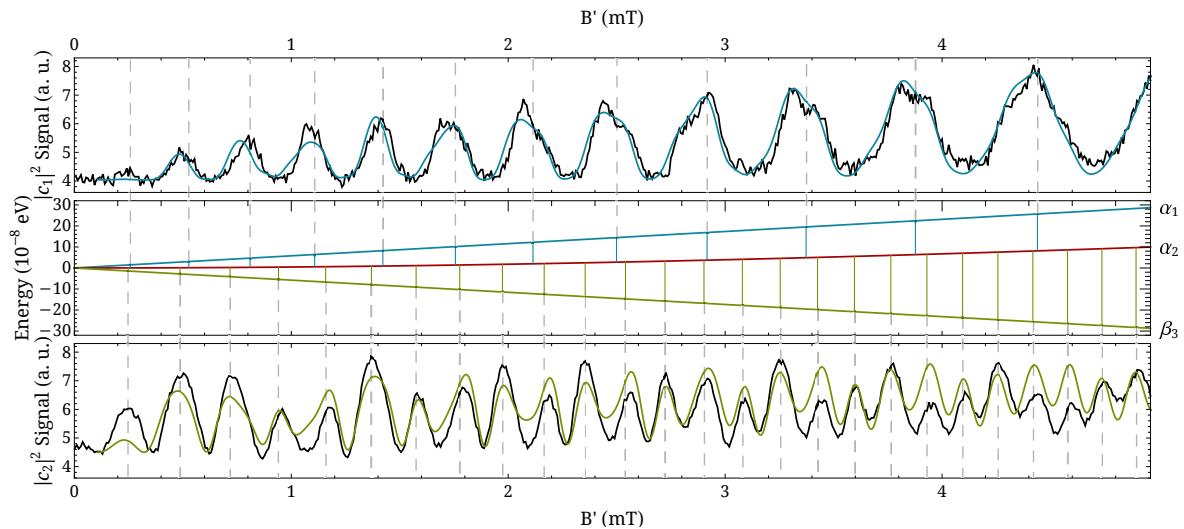


Fig. 4. Simulated (colored) and measured (black) occupation numbers of α_1 and α_2 states for velocity $v = 4.95 \times 10^5$ m/s. The middle plot is the Breit-Rabi diagram for metastable hydrogen.

An alternative way to explain the effect that takes place in the Sona transition unit is the following. The atoms are transferred from the α_1 state to the β_3 due to the inversion of the B_z direction. In parallel, they experience a time-varying radial component with a definite shape, but an increasing amplitude with distance from z -axis (see Eq. (1)). The last induces transitions from β_3 to α_2 and from α_2 to α_1 . Equivalently, multiple photons of frequency f are absorbed, which correspond to energy differences

$$\Delta E = n \cdot h \cdot f, \quad (5)$$

where n denotes an integer number. The frequency f depends on the shape of the radial magnetic field (viz. distance between Sona coils) and the velocity of the hydrogen atoms. The Breit-Rabi diagram

in Fig. 4 shows the positions where integer multiples of $f = 3.536$ MHz are found. We introduce the averaged magnetic field B' for our description, since the field in the Sona coils is not constant (Fig. 3). It is related to the maximum field by $B' = (0.723 \pm 0.003) B_{max} + (0.004 \pm 0.020)$ mT, which is obtained by analyzing the measured signals. In this way, $\Delta E_{n=1} = (14.62 \pm 0.03)$ neV or $f_1 = (3.536 \pm 0.007)$ MHz was determined with the current setup [12].

4. Conclusion and Future Work

The wavelength λ of the hyperfine transitions is evaluated from the equation

$$v = \lambda \cdot f \quad (6)$$

and is determined by the shape of the radial magnetic field component. This parameter can be tuned to decrease further the uncertainty ($\Delta E = 3 \times 10^{-11}$ eV or $\Delta f = 7$ kHz). In addition, the replacement of the electron-impact ionizer with an ECR (electron-cyclotron resonance) ion source will provide proton beams up to 20 μ A and offer better statistics. Further improvements to the magnetic field shielding will contribute to the reduction of the uncertainty.

Moreover, different methods for data analysis are currently being investigated. These include the concept of odd integer multiples of the fundamental frequency and the consideration of two calibration functions for B' (one for each α state) due to the difference in the effect of the second spinfilter to the Sona field. The reason for this is that the magnetic field in the second spinfilter needs to change for the two measurements and this change influences the Sona field.

The aim is to decrease the statistical uncertainty down to 10^{-13} eV, where the QED corrections [13] in the Breit-Rabi formula can be tested. Similar measurements with an improved experimental setup are also planned for deuterium atoms.

Acknowledgements

The work has received funding from the ATHENA project of the Helmholtz Association (HGF). Lukas Huxold acknowledges support by the Deutsche Forschungsgemeinschaft within project BU 2227/1-1.

References

- [1] P. G. Sona, *Energia Nucleare* **14**, 295 (1967).
- [2] N. Kolachevsky, A. Matveev, J. Alnis, C. G. Parthey, S. G. Karshenboim, and T. W. Hänsch, *Phys. Rev. Lett.* **102**, 213002 (2009).
- [3] N. Kolachevsky, P. Fendel, S. G. Karshenboim, and T. W. Hänsch, *Phys. Rev. A* **70**, 062503 (2004).
- [4] A. Kponou, A. Zelenski, S. Kokhanovski, and V. Zubets, *AIP Conf. Proc.* **980**, 241 (2008).
- [5] E. Antishev, and A. Belov, *AIP Conf. Proc.* **980**, 263 (2008).
- [6] A. Zelenski, J. G. Alessi, A. Kponou, and D. Raparia, *Proc. 11th Eur. Part. Accel. Conf.*, Genoa, Italy, 2008, p. 1010.
- [7] P. Buske, B. S. Thesis, RWTH Aachen University, Aachen (2016).
- [8] Y. Gan, B. S. Thesis, FH Aachen, Jülich (2017).
- [9] J. McAndrew, S. Paul, R. Emmerich, R. Engels, P. Fierlinger, M. Gabriel, E. Gutsmedl, J. Mellenthin, J. Schön, W. Schott, A. Ulrich, F. Grünauer, and A. Röhrmoser, *Hyperfine Interact.* **210**, 13 (2012).
- [10] W. Schott, E. Gutsmedl, K. Bernert, R. Engels, R. Gernhäuser, S. Huber, I. Konorov, B. Märkisch, S. Paul, C. Roick, H. Saul, and S. Spasova, *EPJ Web Conf.* **219**, 04006 (2019).
- [11] R. Engels, R. Emmerich, G. Tenckhoff, H. Paetz gen. Schieck, M. Mikirtychiants, F. Rathmann, H. Seyfarth, and A. Vassiliev, *Rev. Sci. Instrum.* **74**, 4607 (2003).
- [12] R. Engels, M. Büscher, P. Buske, Y. Gan, K. Grigoryev, C. Hanhart, L. Huxold, C. S. Kannis, A. Lehrach, H. Soltner, and V. Verhoeven, *Eur. Phys. J. D* **75**, 257 (2021).
- [13] D. L. Moskovkin, and V. M. Shabaev, *Phys. Rev. A* **73**, 052506 (2006).